Supporting Information for

Emissions from an international airport increase particle number concentrations fourfold at 10 kilometers downwind

N. Hudda[1], T. Gould[2], K. Hartin[3], T. Larson[2], and S.A. Fruin[1]*†

[1]Keck School of Medicine, Department of Preventive Medicine, University of Southern California, Los Angeles, CA 90089, United States
[2]Department of Civil and Environmental Engineering, University of Washington, Seattle, WA 98195, United States
[3]Department of Environmental and Occupational Health Sciences, University of Washington, Seattle, WA 98195, United States

Corresponding Author
*Telephone: 323-442-2870. Fax: 323-442-3272. E-mail: fruin@ usc.edu.

Present Address
†S. A. Fruin: Department of Preventive Medicine, University of Southern California, 2001 North Soto Street, Los Angeles, CA 90089-9013, United States

Number of Pages: 19

Number of Figures: 11

Number of Tables: 3

List of Figures

List of Tables

MONITORING AREA

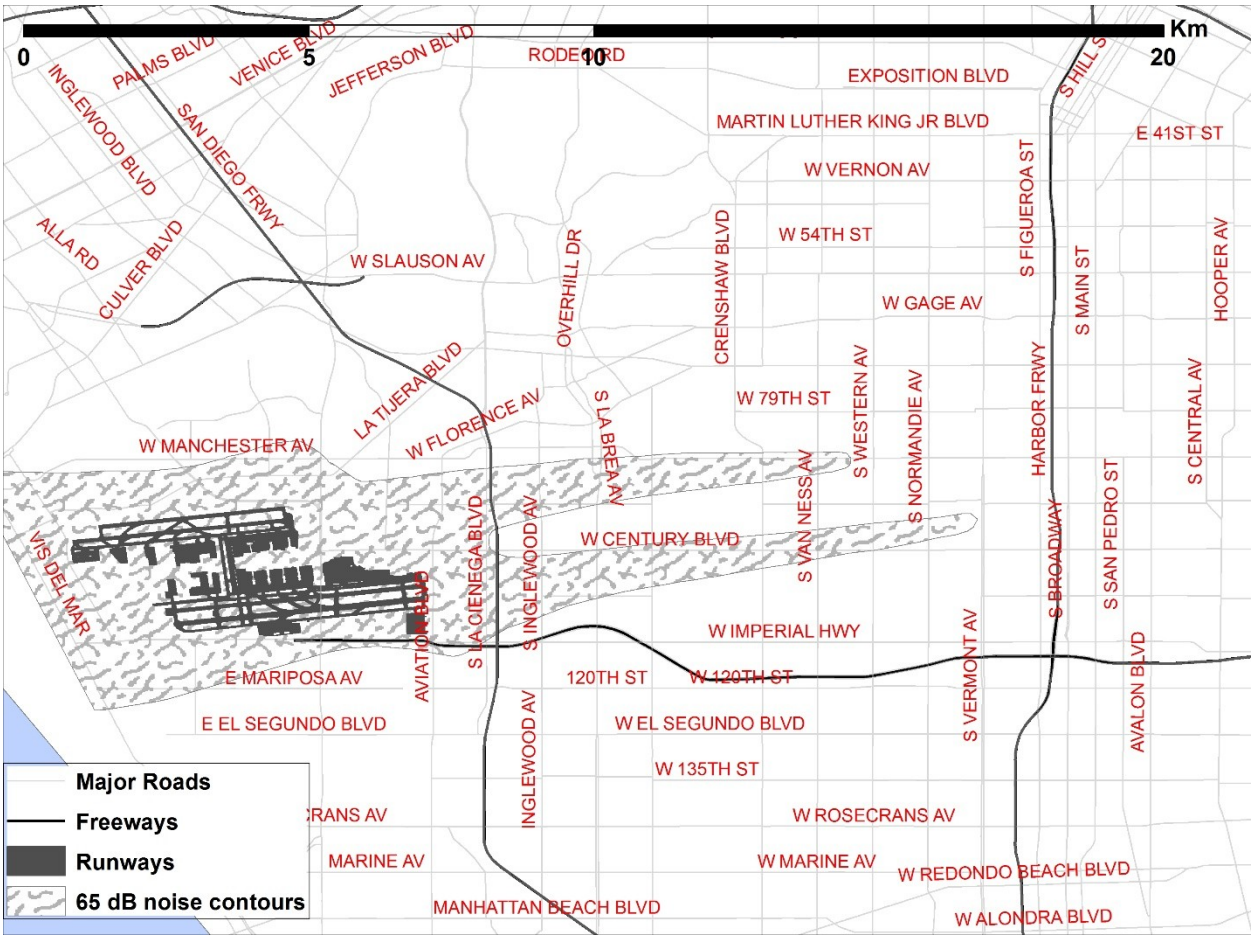

Figure S.1: Map of the area around LAX with major street name labels.

INSTRUMENTS

Table S.1: Instruments used in University of Southern California Mobile Monitoring Platform

Instrument	Parameter measured	Instrument Flow Rate (L min^{-1})	Response Time (s)	Accuracy, Resolution, Sensitivity	Detection Limit
TSI portable CPC (ethanol-based) model 3007	Particle number (PN) conc., 10 nm–1 um	0.8	<9 sec for 95% response	20%, 1 particle/cm^3, -	10 nm, <0.01 particles/cm^3
Aeth Labs MicroAeth AE 51 Model Year 2010	Black carbon (BC)	0.15	~5	±0.1 µg BC/m^3, 0.001 µg BC/m^3, -	±0.1 µg BC/m^3 at 1 min avg
EcoChem PAH analyzer, model PAS 2000	Particle-bound polycyclic aromatic hydrocarbons (PB-PAH) and elemental carbon	2	< 10	- - 0.3–1 ng /m^3 PB-PAH per picoamp	3 ng/m^3
Garmin GPSMAP 76CSx	Location, speed	N/A	1	3 meters - -	
2-B Technology Model 401-410	NO_X	1	8	Higher of 1.5 ppb or 2% of reading	

Table S.2: Instruments used in University of Washington Mobile Monitoring Platform

Instrument	Parameter measured	Instrument Flow Rate (L min^{-1})	Response Time (s)	Accuracy, Resolution, Sensitivity	Detection Limit
TSI portable CPC (Ethanol-based) model 3007	Particle number(PN) conc., 10 nm–1 um	0.8	<9 sec for 95% response	20%, 1 particle/cm^3, -	10 nm, <0.01 particles/cm^3
Aeth Labs Micro Aeth AE 52	Black carbon (BC)	0.20	~5	±0.1 µg BC/m^3, 0.001 µg BC/m^3, -	±0.1 µg BC/m^3 at 1 min avg
Aerodyne CAPS NO_2 monitor	NO_2	0.85	~8	0.01 ppb - -	< 0.1 ppb
US GlobalSat BU-353 GPS	Location, speed	N/A	0.1	Location: 5 m - -	

WIND ROSES

The following wind roses describe the distribution of wind speed and direction for the results shown in Figure 2–3. The wind roses were based on data collected by Automated Surface Observing Systems monitor operated by National Weather Service at site KLAX located at LAX and reported as 2 minute averages at 1 minute resolution. (The wind speed summary in Table 1 of the manuscript is based on hourly data.)

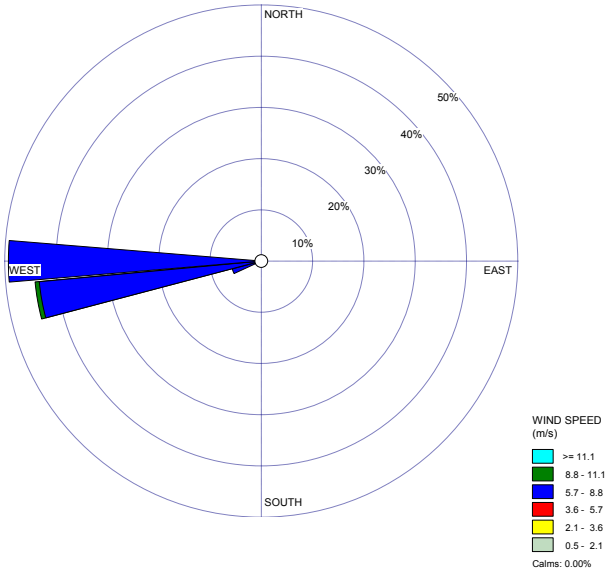

Figure S.2 (a): Wind rose for 1300–1459 hours, Sep 29, 2012.

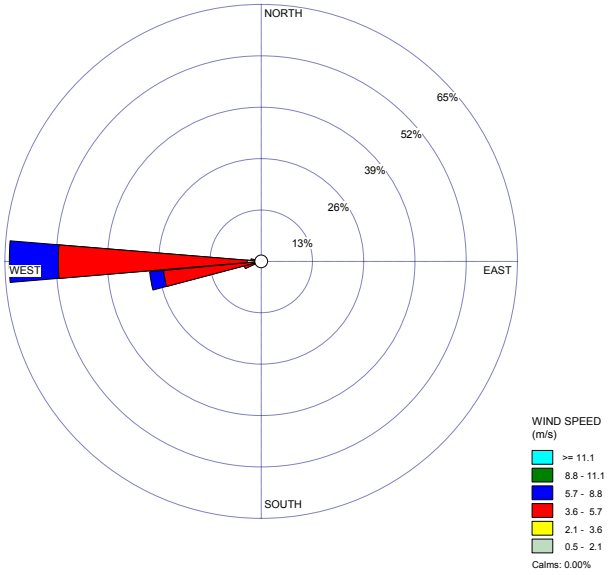

Figure S.2 (c): Wind rose for 1630–1820 hours, Sep 30, 2012.

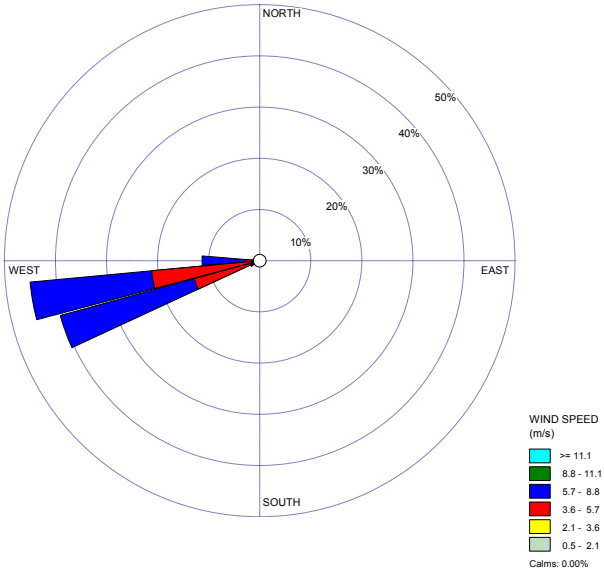

Figure S.2 (b): Wind rose for 1500–1730 hours, Sep 29, 2012.

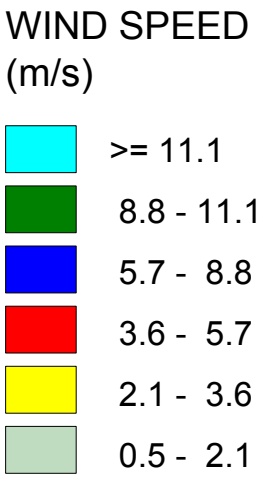

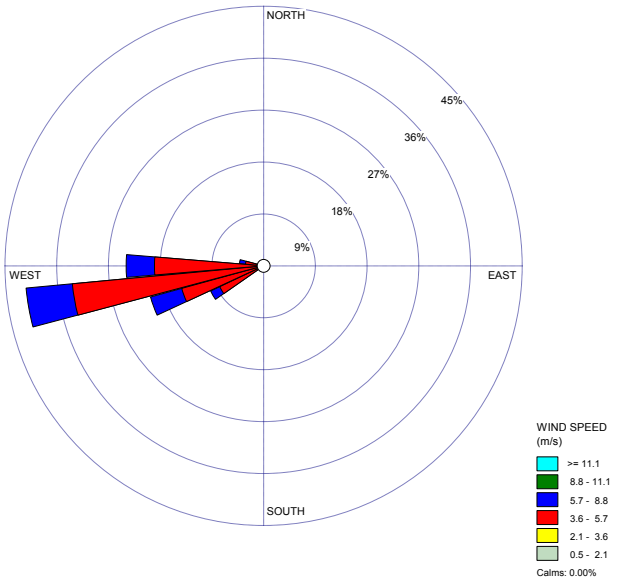

Figure S.2 (d): Wind rose for 1200–1830, Jun 22, 2013.

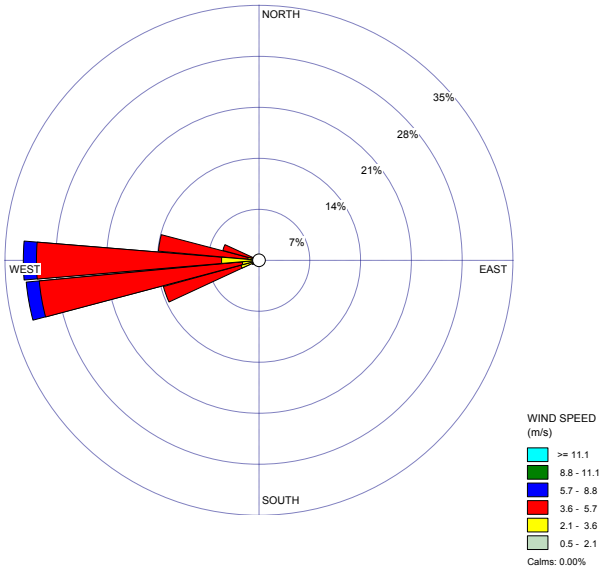

Figure S.2 (f): Wind rose for 0931–1559, Jul 01, 2013.

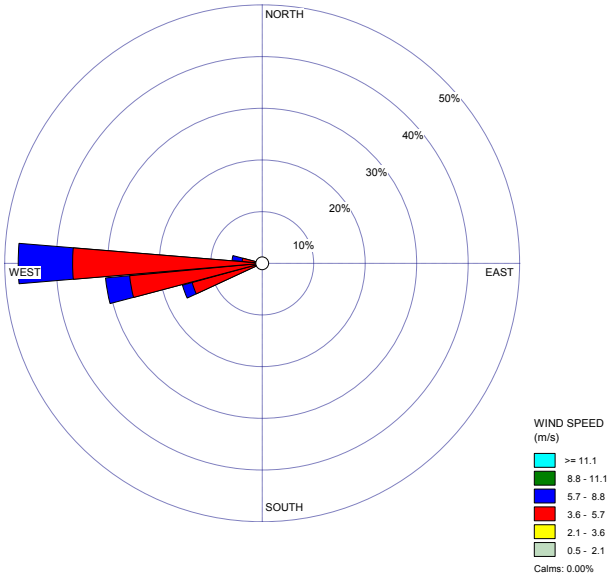

Figure S.2 (e): Wind rose for 1200–1615, Jun 27, 2013.

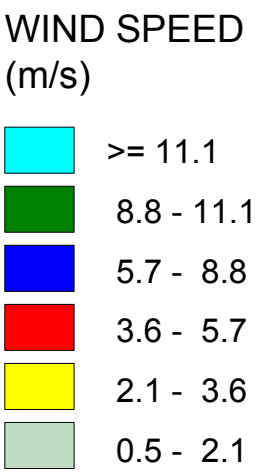

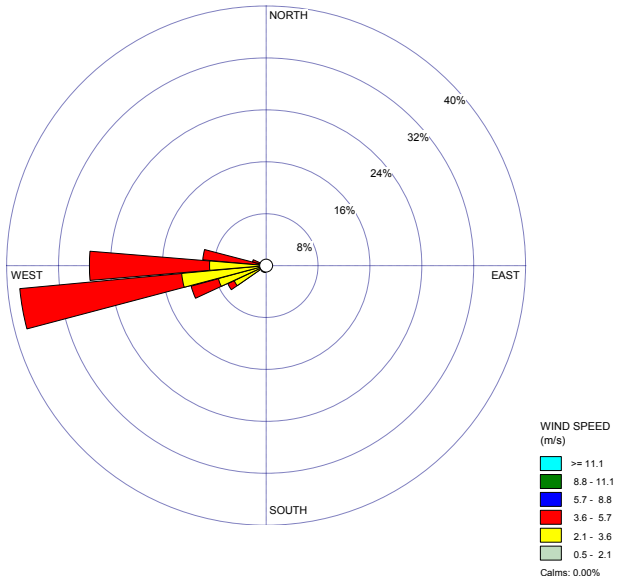

Figure S.2 (g): Wind rose for 0850–1450, Aug 15, 2013.

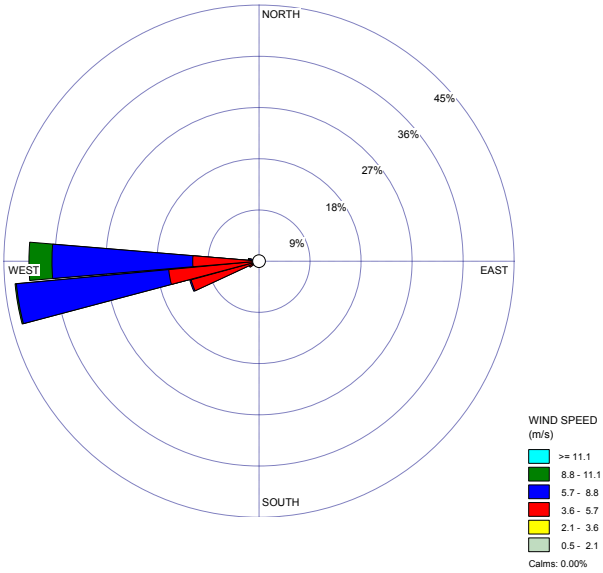

Figure S.2 (h): Wind rose for 1100–1759, Aug 23, 2013.

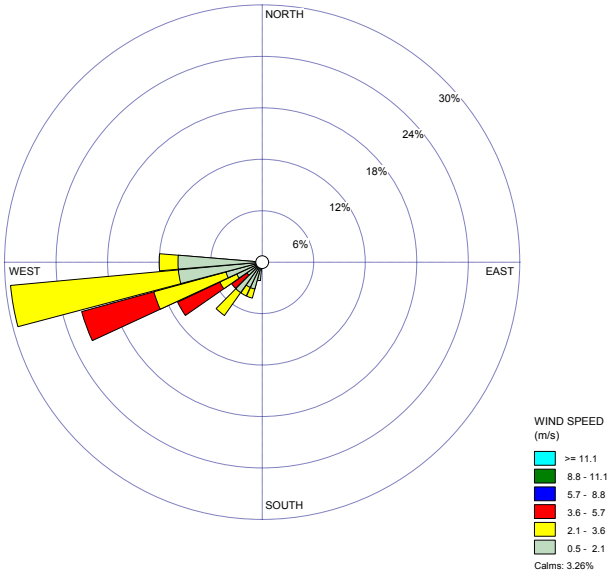

Figure S.2 (i): Wind rose for 1923–2359, Aug 23, 2013.

Wind Roses for spring-winter sampling data presented in Figure S.8 and S.9 in this Supporting Information are presented in Figures S.3 (a)–(g).

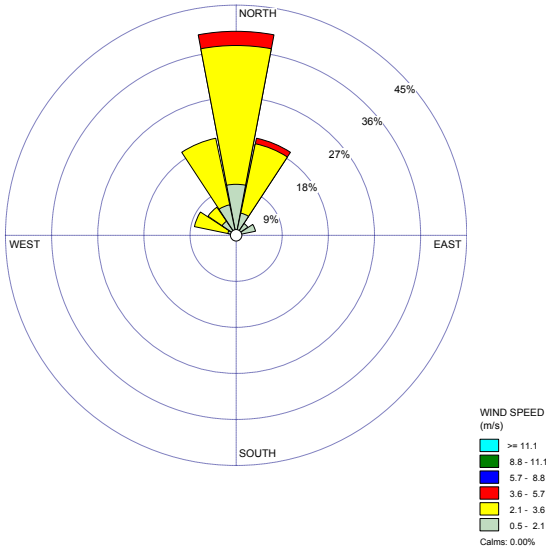

Figure S.3 (a): Wind rose for 1830–2100 hours on Dec 10, 2013.

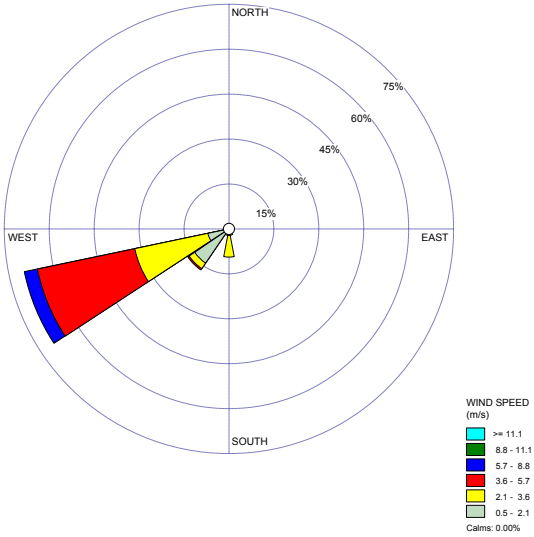

Figure 3 (b): Wind rose for 1645–1845 hours Dec 18, 2013.

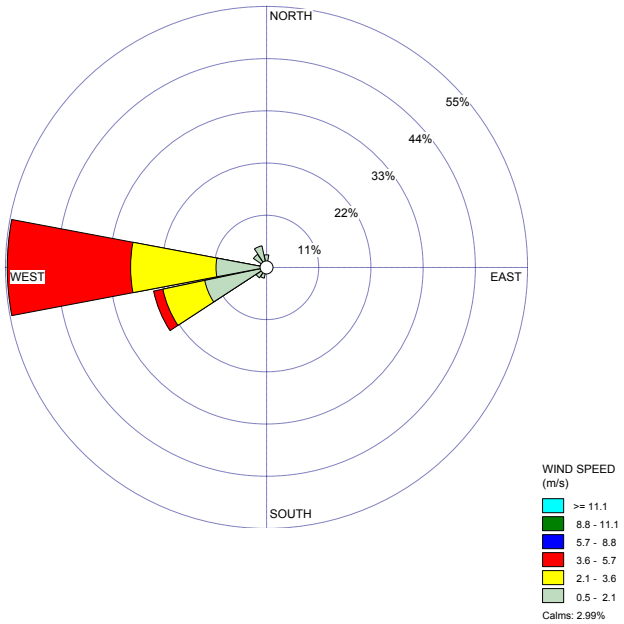

Figure S.3 (c): Wind rose for 1500–2000 hours on Dec 23, 2013.

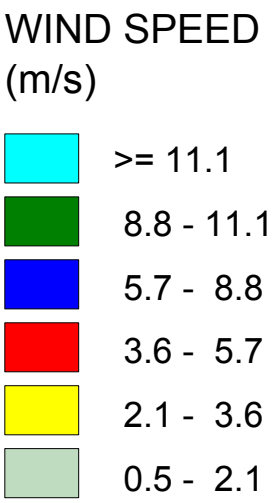

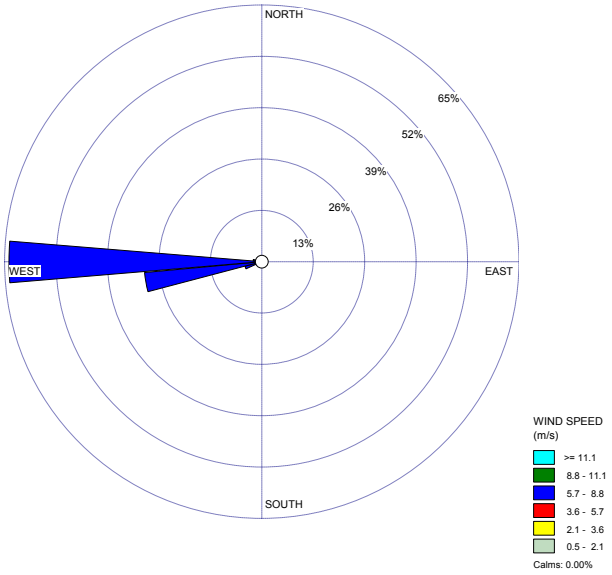

Figure S.3 (d): Wind rose for the sampling duration on Apr 10, 2011

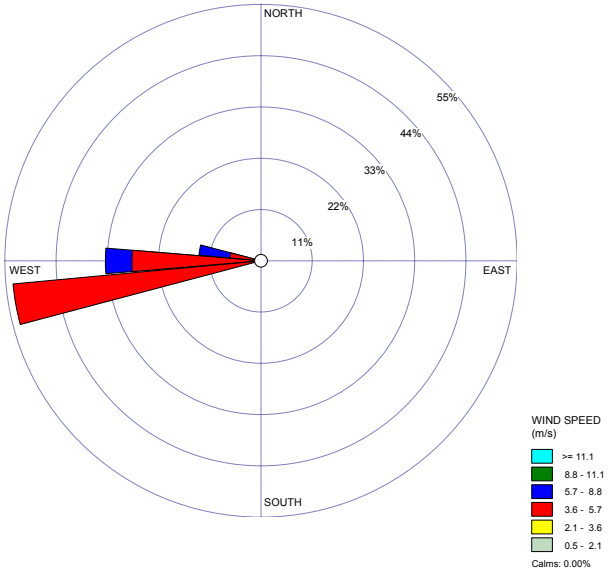

Figure S.3 (d): Wind rose for the sampling duration on Jan 26, 2012

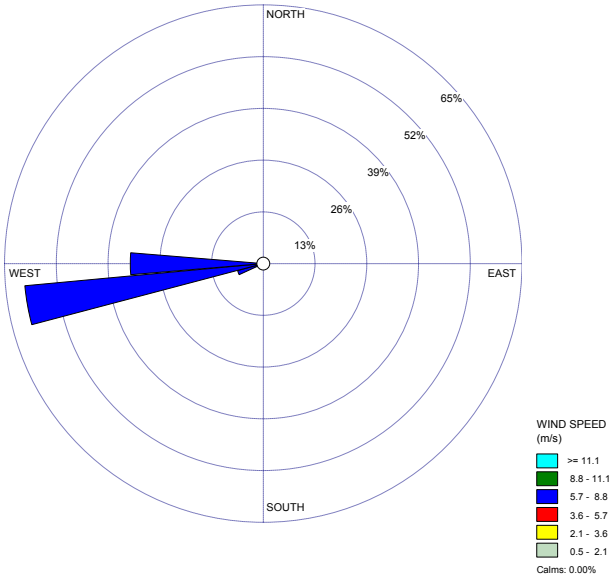

Figure S.3 (f): Wind rose for the sampling duration on May 27, 2011

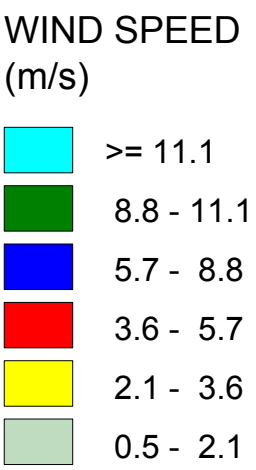

DATA PROCESSING

Figure S.4 shows the raw data that include a localized traffic emissions signal representing microscale (10–100m) and middle scale variations (100 – 500m) and the underlying "baseline" pollutant concentration that only varied gradually over the neighborhood scale (500 m–4 km). Local traffic emissions were excluded by taking a rolling 30-second 5th percentile value of the 1-second concentration time series, and assigning that value to the measured location, resulting in a smoothed data series of 1 s data which we referred to as "baseline." The figure illustrates that this data smoothing process successfully captures the broader spatial-scale changes while removing the transitory and localized impacts of specific vehicles on the roadways sampled. Occasionally, individual spikes/plumes lasted longer than 30 seconds. In those rare instances, the spikes were excluded manually if confirmed to be a specific vehicle by video or field-notes.

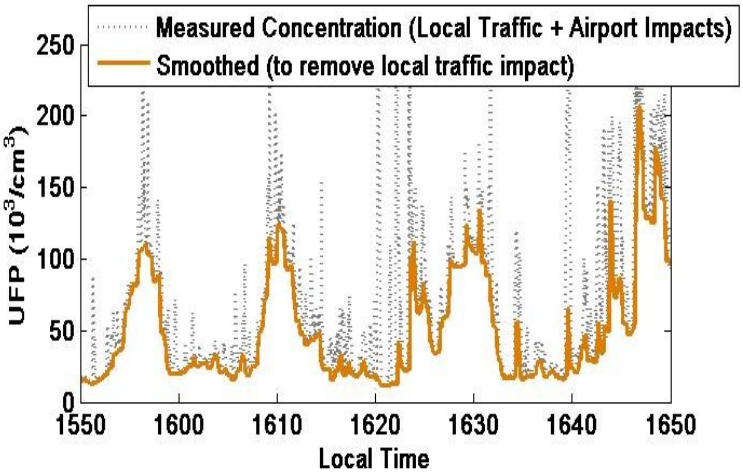

Figure S.4: Illustration of data before and after smoothing

The following figures illustrate that the smoothed data series retained the neighborhood-scale changes in baseline PN concentrations occurring over several kilometers as shown in Figure S.5. Figure S.6 shows PN concentration versus distance from the start of the transects labeled in Figure S.5. Figure S.7 shows same PN concentration profile plotted versus monitoring time. These PN concentration profiles for selected transects from monitoring from 17:30 on 08/24/2013 to 01:00 on 08/25/2013 show that this increase in PN baseline concentration occurred over a scale of kilometers. The longer duration spikes that weren't manually removed do not obscure the spatial pattern. Even as far downwind as 10–16 km, the increase was easily discernible in real time at arterial road driving speeds (e.g., over 5–10 minutes per transect at 32–56 km/h speeds).

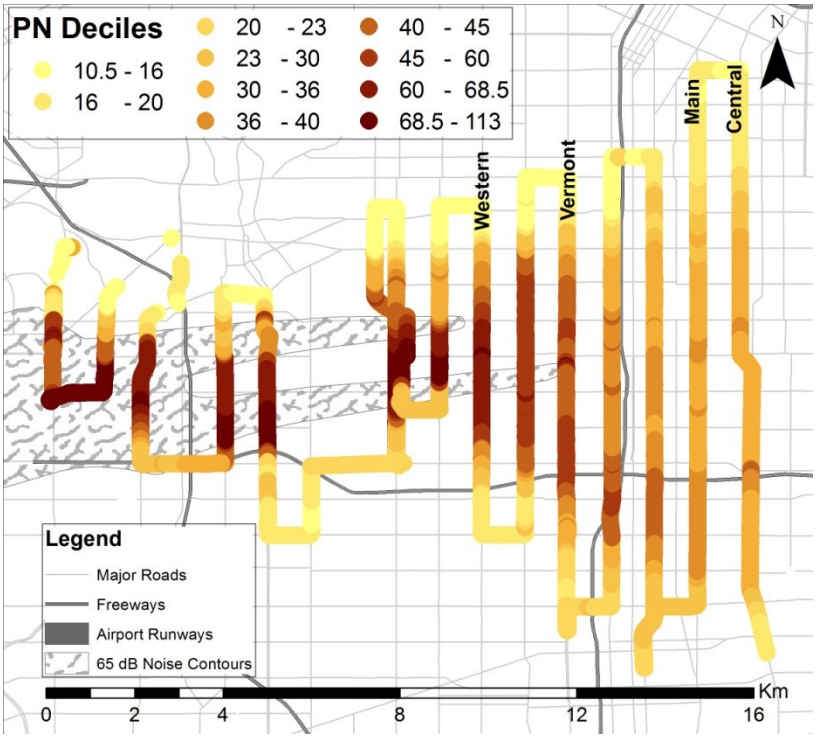

Figure S.5: Spatial pattern of the PN concentration monitoring from 17:30 08/24/2013 to 01:00 08/25/2013 including the transects shown below.

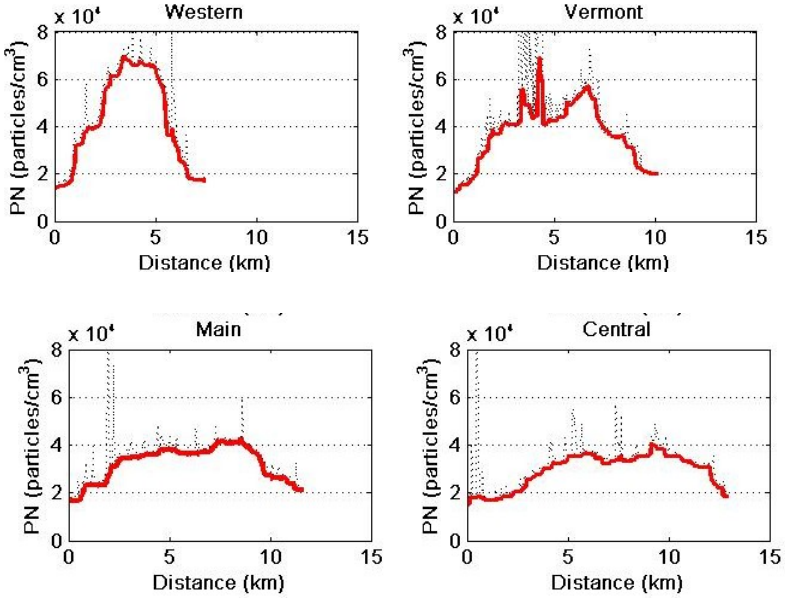

Figure S.6: Raw data (black line) and smoothed data (red line) for transects on Western (10 km east of LAX), Vermont (11.75 km east of LAX), Main (13.5 km east of LAX) and Central Av. (16 km east of LAX).These transects have been identified with street name labels in Figure S.5.

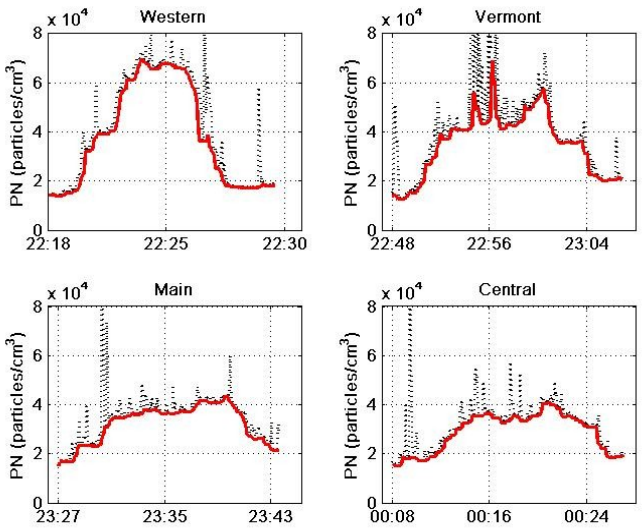

Figure S.7: Raw data (black line) and smoothed data (red line) time-series for transects on Western (10 km east of LAX), Vermont (11.75 km east of LAX), Main (13.5 km east of LAX) and Central Av. (16 km east of LAX). These transects have been identified with street name labels in Figure S.5.

TRAFFIC VOLUMES

A major thoroughfare in Los Angeles, Freeway I-405, runs N-S at the eastern edge of LAX. Freeway 105 runs E-W at the southern edge of LAX but traffic volumes are smaller on I-105 than on I-405. Where I-105 crosses I-405, the annual average daily traffic count (AADT) in 2012 for I-105 was 177,500 vehicles per day (both directions) with a truck fraction of 4.8%, and for I-405, 274,000 vehicles per day with a truck fraction of 3.3 %. Where I-105 crosses I-110, which runs N-S about 12 km east of LAX and closer to the eastern extent of the study area, the AADT increases to 231,000 vehicles per day with a truck fraction of 5.2% for I-105 and an AADT of 269,500 and 4.3%, respectively, for I-110.

SPATIAL PATTERN OF PN ELEVATION ON ADDITIONAL WINTER DAYS

Figure S.8 shows the pattern during additional winter days with different prevailing wind directions. For the corresponding wind roses see Figures S.3 (a)–(c). The prevailing wind direction was northerly on 12/10/2013, southwesterly on 12/18/2013 and westerly on 12/23/2013. The impacted locations corresponded to the wind direction but impacted PN concentrations were comparable, except for the baseline that was higher under northerly wind because it was influenced by urban air and not the usual marine air associated with westerly/southwesterly wind.

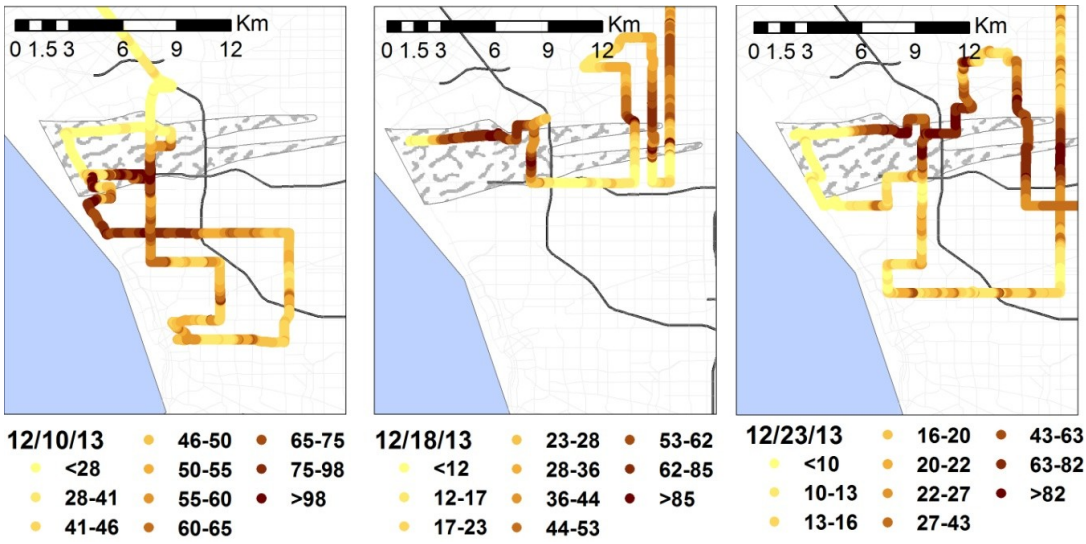

Figure S.8: Spatial pattern of impact during monitoring in December 2013. PN concentrations are colored by deciles and plotted in units of 1000 particles/cm^3.

SPATIAL PATTERN OF PN ELEVATION IN PREVIOUS YEARS

Archived records from previous years were re-examined to uncover similar impacts from LAX. Figure S.9 shows the spatial pattern of PN concentration increase on two transects Western Av which is 10 km east of LAX and Avalon Av. which is 14 km east of LAX. These runs were conducted in winter and spring time of 2011 and 2012.

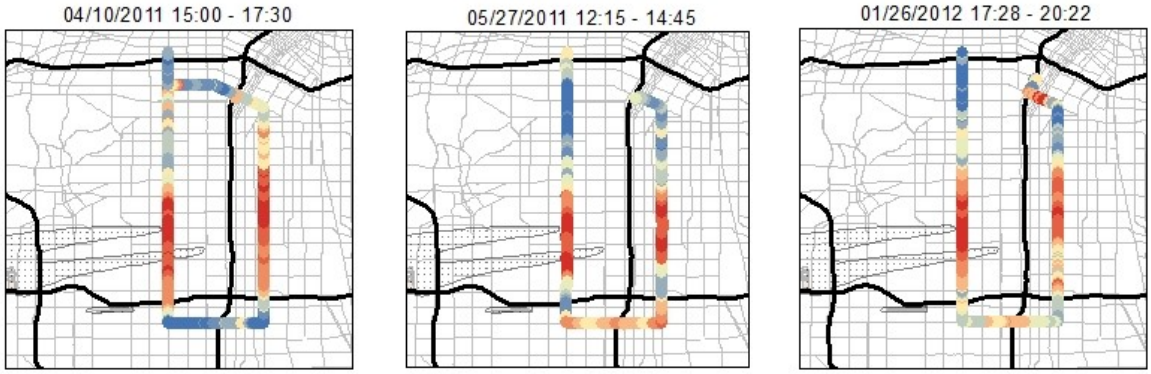

Percentile	4/10/2011	5/27/2011	1/26/2012
10	7750	10000	18200
20	8980	11400	20400
30	10600	13600	22300
40	11600	15500	23900
50	13300	18800	25600
60	14600	25800	29600
70	17800	28000	36800
80	22900	31400	43000
90	35000	39500	53500
100	55500	53900	137700

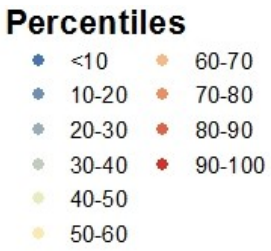

Figure S.9: Spatial pattern of PN concentration during monitoring in 2011 observed on Western Av (10 km east of LAX) and Avalon Av. (14 km east of LAX).

CONCURRENT SAMPLING

The use of two mobile platforms allowed us to measure the pollutant concentrations at two locations concurrently and further verified the high temporal and spatial consistency of the impacts. During these runs, the USC MMP monitored within 7.5 km of LAX and the UW MMP monitored 9.5–12 km from LAX.

To ensure neither mobile platform was affected by its own emissions, the USC MMP hybrid vehicle engine turned off when the car was not moving. For the UW MMP, a regular gasoline powered van, the sampling inlet location was located at about five feet high through the second row passenger window behind the driver, away from the tailpipe location at the other side of the vehicle under the rear. This orientation prevented the tailpipe from being upwind of the sampling inlet during the north and south transects. They were driven at similar speeds to cover the same N-S distance within the same time via synchronous crossing of major E-W cross streets. During this dual mobile platform monitoring, transects were sampled multiple times within a short span of time. No direct comparisons were made between the data from two platforms and this sampling was conducted only to measure the consistency in spatial patterns. (The two CPC agreed within 10% during collocated sampling before and after the run.)

The profiles shown in Figure S.10 (a), (c) and (d) for a given transect were remarkably consistent over the duration of one to two hours. The overall spatial pattern is illustrated in Figure S.10 where successive loops on the monitoring route are staggered in the northeast direction. The pattern between measured by two MMPs but at different locations aligned well with the prevailing winds for that day, which is shown in Figure S.11.

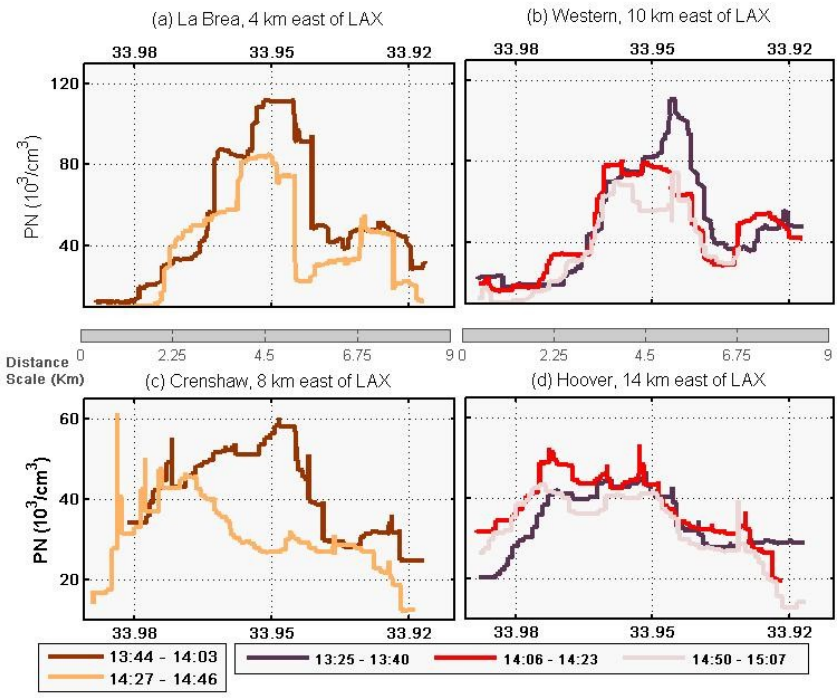

Figure S.10: PN concentrations on multiple consecutive transects.

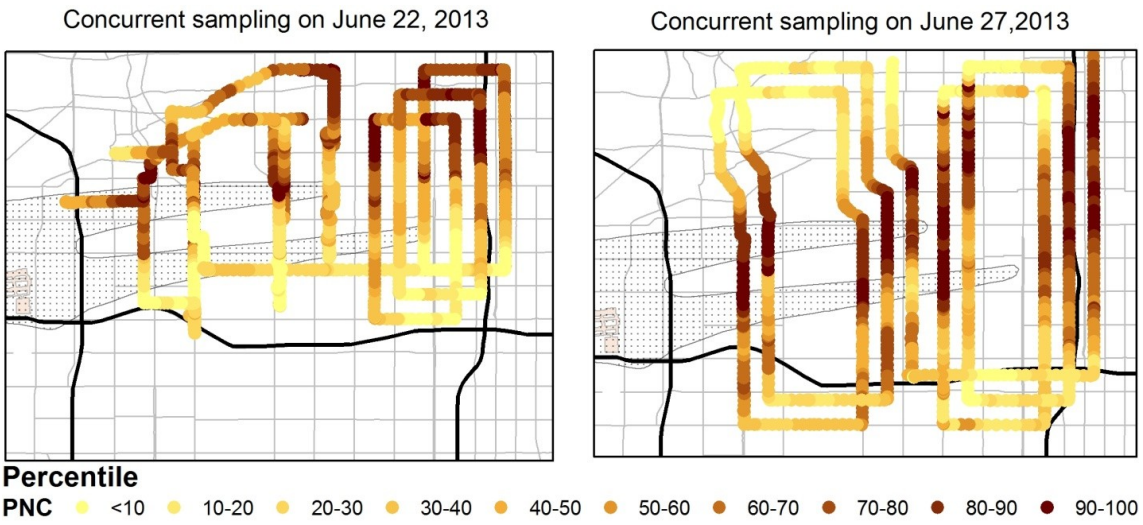

Figure S.11: Spatial pattern (staggered for visibility) for PN concentrations on concurrent sampling runs of June 22 and June 27. Western loops were sampled with the USC MMP and eastern loops with the UW MMP.

CALCULATIONS FOR COMPARING FREEWAY IMPACTS

The following tables present the detailed calculations used to calculate the length of freeway necessary to produce the equivalent area-weighted increases in PN concentration produced by LAX. Table S.3(a) gives the area-weighted PN concentration increases for each 10,000/cm3 step in PN concentration for each of the three days. Table S.3(b) gives the area-weighted PN concentration increases for each 10 meter interval downwind of a typical freeway in Los Angeles. Table S.3(c) gives the figures used to calculate the equivalent freeway distances.

Table S.3(a): Average LAX-related particle number increase and corresponding impact areas

8/15/2013 Baseline PN Conc. = 20000/cm^3	Area (km^2)	4	9	14	27	44	65*
	Minimum PN conc. increase in area over baseline (particles/cm^{-3})	70000	60000	50000	40000	30000	20000
	Average conc. increase in area over baseline(particles/cm^{-3})	78700	69100	623000	51300	43200	35600
	Impact (Avg. conc. increase X area), [particles/cm^3 x km^2]	3.15E+05	6.22E+05	8.72E+05	1.39E+06	1.90E+06	2.31E+06*
8/23/2013 Baseline PN Conc. = 20000/cm^3	Area (km^2)	0.1	0.5	7	22	36	47*
	Minimum PN conc. increase in area over baseline(particles/cm^{-3})	70000	60000	50000	40000	30000	20000
	Average conc. increase in area over baseline(particles/cm^{-3})	70000	61400	50700	43600	38200	33700
	Impact (Avg. conc. increase X area), [particles/cm^3 x km^2]	7.00E+03	3.07E+04	3.55E+05	9.58E+05	1.38E+06	1.58E+06*
8/24/2013 Baseline PN Conc. = 15000/cm^3	Area(km^2)	0.5	1.4	4	12	17	30*
	Minimum PN conc. increase in area over baseline(particles/cm^{-3})	70000	60000	50000	40000	30000	20000
	Average conc. increase in area over baseline(particles/cm^{-3})	75800	69200	60200	49800	45100	36500
	Impact (Avg. conc. increase X area), [particles/cm^3 x km^2]	3.79E+04	9.68E+04	2.41E+05	5.97E+05	7.67E+05	1.10E+06*

*Values reported in the research article.

Table S.3(b): Calculations showing increase in particle number concentration from freeways as a function of downwind distance

Distance from freeway (X) † (m)	[a]Conc. increase at distance X for background = 15,000 (particles/cm^3)	Cumulative impact (avg. conc. increase X area) for 1 km of freeway length (particles/cm^3 × km^2)	[a]Conc. increase at distance X for background = 20,000 (particles/cm^3)	Cumulative impact (avg. conc. increase X area) for 1 km of freeway length (particles/cm^3 × km^2)
0-10	56000[b]	560	51000[b]	510
10-20	48200	1040	43900	950
20-30	43600	1480	39700	1350
30-40	39500	1870	36000	1710
40-50	35700	2230	32500	2030
50-60	32300	2553	29400	2330
60-70	29200	2850	26600	2590
70-80	26500	3110	24100	2830
80-90*	23900	3350	21800	3050*
90-100	21700	3570	19700	3250
100-110	195600	3760	17800	3420
110-120	17700	3940	16100	3590
120-130*	16000	4100*	14600	3730
130-140	14500	4250	13200	3870
140-150	13100	4380	12000	3990
150-160	11900	4500	10800	4090
160-170	10800	4600	9800	4190
170-180	9700	4700	8900	4280
180-190	8800	4790	8000	4360
190-200	8000	4870	7300	4430

† For the first 10 m, it is assumed that concentration equals freeway concentration. For distance intervals the values have been reported at the mid-point to nearest 100 particles/cm^3.
*Values reported in the research article

[a]Zhu et al. 2008 (a) regression fit: Particle conc. increase at distance X = (Particle conc. increase on-freeway) × exp (-0.01*X)
[b] Li et al. 2013 Average particle concentration on Los Angeles freeways, i.e., 71,000 particles/cm^3 minus background

Table S.3(c): Calculations showing equivalent freeway lengths

Date	Urban Background	LAX-related impact			Freeway-related Impact, per km of freeway			Equivalent Freeway Length
	(particles/cm^3)	Area (km^2)	Average PN Increase (particles/cm^3)	Impact (particles/cm^3 × km^2)	Area (km^2)	Average PN Increase (particles/cm^3)	Impact (particles/cm^3 × km^2)	(km)
8/15/13	20000	65*	35600	2.31E+06*	0.090	32500*	2930*	790*
8/23/13	20000	47	33700	1.58E+06*	0.090	32500*	2930*	540
8/24/13	15000	30*	36500	1.10E+06*	0.130	30200*	3930*	280*

*Values reported in the research article